Journal of Inclusion Phenomena and Molecular Recognition in Chemistry **32:** 91–102, 1998.

An Unusual Mixed-guest Inclusion Compound. Crystal Structures of the Host Compound Hexakis(3-hydroxy-3,3-diphenylprop-2-ynyl)benzene, and its Inclusion Compound with Acetonitrile and Benzene

SUSAN A. BOURNE*[,a], KATHERINE L. GIFFORD NASH[a] and FUMIO TODA[b]

[a]*Department of Chemistry, University of Cape Town, Rondebosch, 7701, South Africa.* [b]*Department of Applied Chemistry, Faculty of Engineering, Ehime University, Matsuyama 790, Japan.*

(Received: 23 September 1997; in final form: 2 December 1997)

Abstract. The crystal structures of the α-phase of hexakis(3-hydroxy-3,3-diphenylprop-2-ynyl)benzene (**1**), and its inclusion compound with acetonitrile and benzene (**2**) have been determined by single crystal diffraction. **2** was further characterised by nuclear magnetic resonance spectroscopy, and thermal analysis. The inclusion of benzene by this host appears to depend on the presence of acetonitrile.

Key words: hexapedal host, α-phase, mixed guest inclusion compound.

Supplementary Data relating to this article are deposited with the British Library. Supplementary Publication No. SUP 82238.

1. Introduction

In the mid-1970's the first systematic design of a new host with no direct structural relationship to any known host was accomplished. These hosts were called 'hexa-hosts' [1]. Since then a number of 'hexa-hosts' have been synthesised and their inclusion behaviour investigated [2]. Hexakis(3-hydroxy-3,3-diphenyl-prop-2-ynyl)benzene, **H**, is proving to be a very successful 'hexa-host' including a number of small volatile organic guests [3–5]. **H** has shown rather complex selectivity, having formed an inclusion compound with 1,3-dioxolan-2-one, which was present in only a trace amount in our sample of 1,3-dioxolane [5]. We suggested that **H** was selective for molecules with a carbonyl oxygen over those with an ether oxygen, even when the former is present in very small amounts. We have been extending this study to examine possible π-intercalators, such as benzene

* Author for correspondence (E-mail: xraysue@psipsy.uct.ac.za; Fax: +27 21 689 7499.

or naphthalene, as well as to determine the effect of nitrogen-hydrogen bond acceptors, for example acetonitrile or pyridine. This has resulted in us encountering another aspect of this host's selectivity. Crystals of **H** grown from benzene are the non-porous α-phase of **H**. A stable acetonitrile inclusion compound cannot be grown, despite many attempts under different conditions. However, **H** dissolved in a mixture of benzene and acetonitrile gives crystals of a stable mixed inclusion compound. These results, the structure of the non-porous α-phase of **H**, **1**, and its inclusion compound with acetonitrile and benzene, **2**, are reported here.

2. Experimental

2.1. CRYSTAL STRUCTURE

Suitable single crystals of the non-porous α-phase of **H** were grown by slow evaporation from a solution of **H** in benzene (**1**). Crystals of **2** were grown unexpectedly from a solution of benzene with a small acetonitrile impurity. A crystal of **1** was mounted on a glass fibre, while **2** was mounted in a Lindemann capillary tube, because the compound is unstable. Preliminary cell dimensions and space group symmetry were determined photographically. Intensity data were collected in the ω-2θ scan mode on an Enraf Nonius CAD4 diffractometer with graphite-monochromated MoK_α radiation (λ = 0.7107Å). The data for **1** was collected at 294 K, whereas **2** was cooled using an Oxford Cryostream cooler and the data collected at 223 K. Three reference reflections were monitored periodically for intensity and orientation control. The data reduction included correction for Lorentz and polarisation effects but not for absorption.

Both structures were solved by direct methods using SHELXS-86 [6], and refined by full-matrix least-squares using SHELXL-93 [7], refining on F^2. All non-hydrogen atoms were refined anisotropically. Hydroxyl hydrogens were located in the difference Fourier maps, and refined isotropically, except for H1O in **1** which was placed in a geometrically calculated position and allowed to refine with an isotropic temperature factor linked to O1. All other hydrogen atoms were placed in geometrically calculated positions.

Crystal data and experimental details are given in Table I.

2.2. THERMAL ANALYSIS

Thermogravimetry (TG) and differential scanning calorimetry (DSC) were performed on a Perkin-Elmer PC7 system. Crystals were removed from the mother liquor, blotted dry and lightly crushed before analysis. Samples of 2–5 mg were analysed over the temperature range 30–300 °C at a heating rate of 10°/min, and with dry nitrogen purge gas flowing at *ca* 40 cm^3 min^{-1} (TG) and *ca* 30 cm^3 min^{-1} (DSC).

Table I. Crystal data and details of structure refinement.

Parameter	**1**	**2**
Molecular formula	$C_{96}H_{66}O_6$	$C_{96}H_{66}O_6.2C_6H_6.2C_2H_3N$
Molecular mass (g.mol^{-1})	1315.57	1553.91
Crystal system	Triclinic	Monoclinic
Space group	$P\bar{1}$	$P2_1/n$
a (Å)	10.683(2)	15.952(2)
b (Å)	11.065(1)	9.144(3)
c (Å)	15.442(3)	29.251(2)
α (°)	99.78(1)	90
β (°)	98.27(1)	89.917(8)
γ (°)	98.90(1)	90
Volume (Å^3)	1750(8)	4267(1)
Z	1	2
Density (calc) (g.cm^{-3})	1.248	1.209
Linear absorption coefficient μ (mm^{-1})	0.077	0.074
F(000)	690	1636
Colour	Colourless	Colourless
Data collection		
Scan width (mm)	0.8 + 0.35 tan θ	0.8 + 0.35 tan θ
Vertical aperture (mm)	4	4
Aperture width (mm)	1.12 + 1.05 tan θ	1.12 + 1.05 tan θ
Temperature (K)	293(2)	223(2)
Size of crystal (mm)	0.44 × 0.44 ×0.40	0.44 × 0.31× 0.31
Range scanned θ (°)	1–25	1–25
Range of indices h, k, l	−12, 12; −13, 13; 0, 18	−19, 19; 0, 10; 0, 34
Reflections measured	6406	8568
Unique reflections	6155	7482
R_{int}	0.018	0.131
Number of reflections observed with		
$I_{rel} > 2\sigma I_{rel}$	3986	4223
Exposure Time (hours)	45.2	57.6
Decay of standard reflections (%)	−2.0	−3.4
Final refinement		
R ($I_{rel} > 2\sigma I_{rel}$)	0.0405	0.0465
wR2 ($I_{rel} > 2\sigma I_{rel}$)	0.1009	0.1095
w*	a = 0.0515, b = 0.32	a = 0.0613, b = 0.62

Table I. Continued.

Parameter	**1**	**2**
S	1.030	1.017
Mean shift / esd	0	0
Max. height in difference Fourier map ($eÅ^{-3}$)	0.146	0.189
Min. height in difference Fourier map ($eÅ^{-3}$)	−0.191	−0.221

* $w = 1/[\sigma^2(F_c^2) + (aP)^2 + bP]$ where $P = (\max(F_o^2, 0) + 2F_c^2)/3$.

2.3. NUCLEAR MAGNETIC RESONANCE

Samples were dissolved in deuterated chloroform. ^1H spectra were recorded at 200 MHz, at 25 °C on a Varian VXR-200 spectrometer with tetramethylsilane as the reference.

2.4. MICROANALYSIS

C, H, N elemental analyses were performed in duplicate on a Carlo Erba elemental analyser Model 1106. Samples were not dried under vacuum, as this could have resulted in loss of the guests.

2.5. X-RAY POWDER DIFFRACTION

Powder patterns were measured using a Philips vertical goniometer with Ni-filtered CuK_α radiation (λ = 1.5418Å), and automatic receiving and divergence slits. Step scans (0.1° 2θ, with 2s counting times) were performed from 6 to 35° 2θ.

The calculated powder pattern of **1** was generated from the single crystal data using LAZY PULVERIX [8].

3. Results and Discussion

The atomic labelling used is shown in Scheme 1. All the bond lengths and angles lie within expected ranges [9].

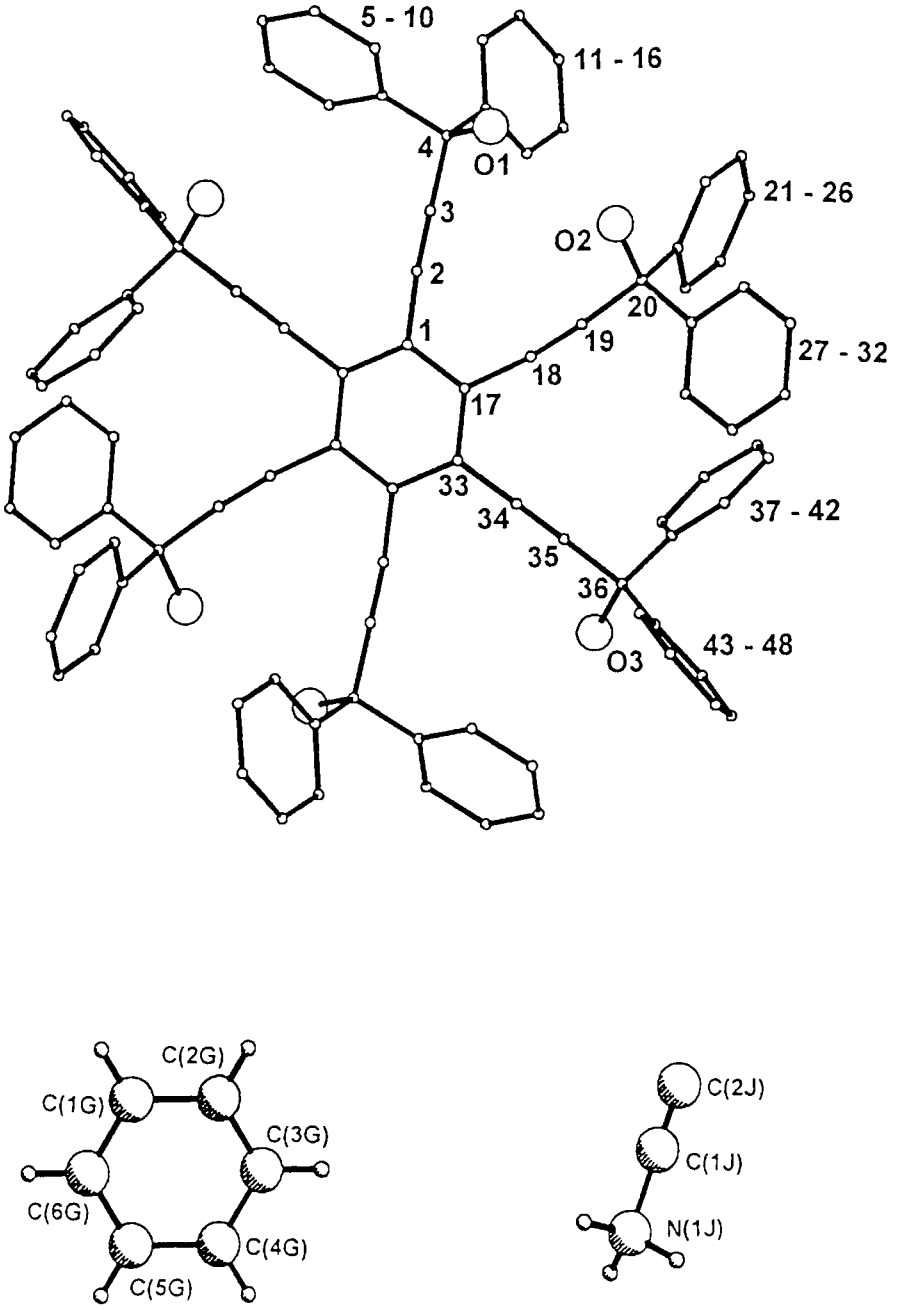

Scheme 1. Atomic labelling scheme used for **H**, and the guest molecules.

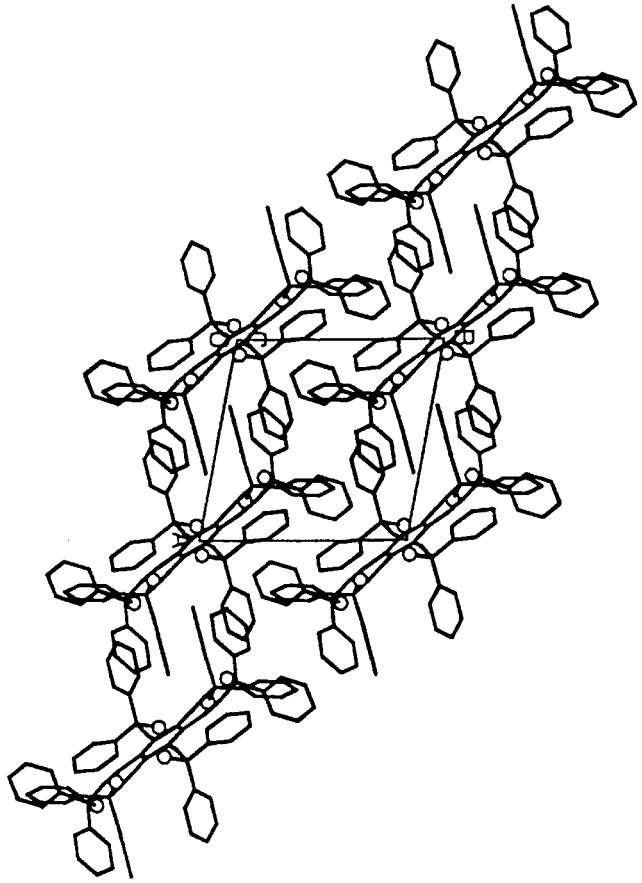

Figure 1. Crystal packing in **1**, viewed down [001].

Table II. Intramolecular hydrogen bond details of **1**.

(D)onor	(A)cceptor	D—H (Å)	D···A (Å)	D—H···A (°)
O3	O1	0.87(3)	3.097(2)	169(3)
O2	Centroid (C37–C42)	1.0(2)	3.611(9)	145(9)

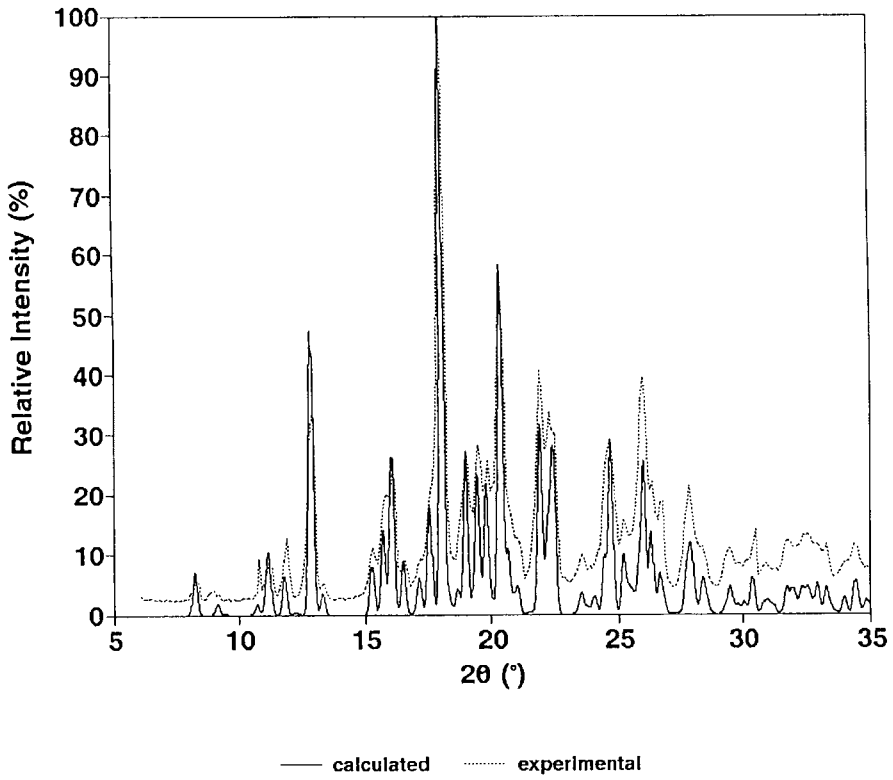

Figure 2. Calculated and experimental XRD powder patterns of **1**.

Table III. Elemental analysis results for **2**.

Element	C	H	O	N
Calculated	86.57	5.45	6.18	1.80
Observed	86.44	5.47	6.33	1.76

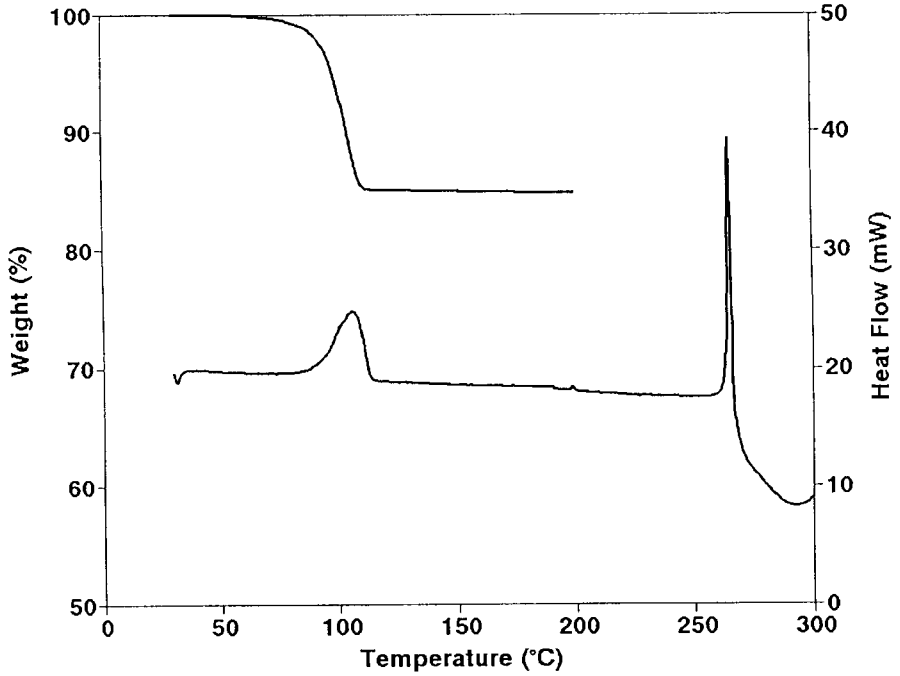

Figure 3. Thermograms (TG and DSC) of **2**.

The non-porous α-phase of **H**, **1**, crystallises in space group $P\bar{1}$. The host molecules pack in layers with the central aromatic ring nearly parallel to the (110) plane, Figure 1. There is no intermolecular O—H···O hydrogen bonding, probably due to the bulky end groups which cause steric crowding around the hydroxyl groups, thereby preventing host to host hydrogen bonding, however, a number of short

Table IV. Hydrogen bond details of **2**.

(D)onor	(A)cceptor	D—H (Å)	D···H (Å)	D—H···A (°)
O3	O2	0.82(3)	2.926(3)	175(3)
O2	N1J	0.96(4)	2.836(4)	172(3)

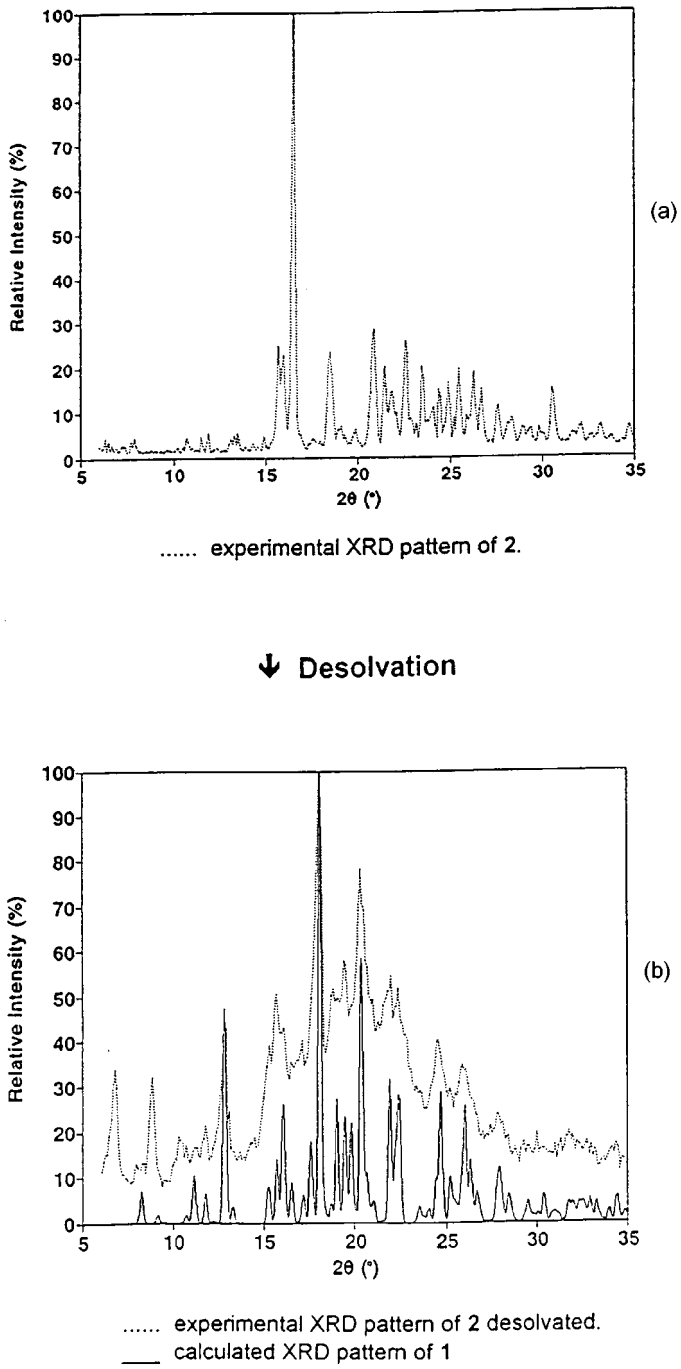

Figure 4. XRD powder patterns of **2** (a) before desolvation, (b) after complete desolvation.

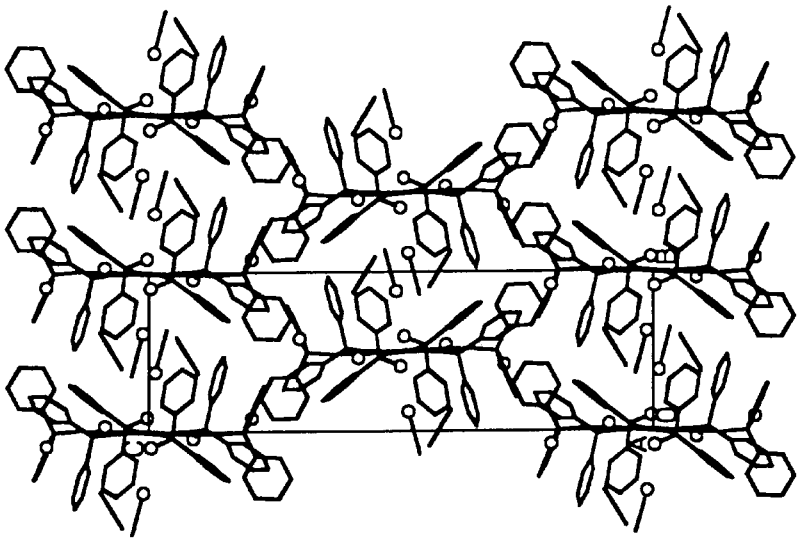

Figure 5. Crystal packing of **2**, viewed along [100].

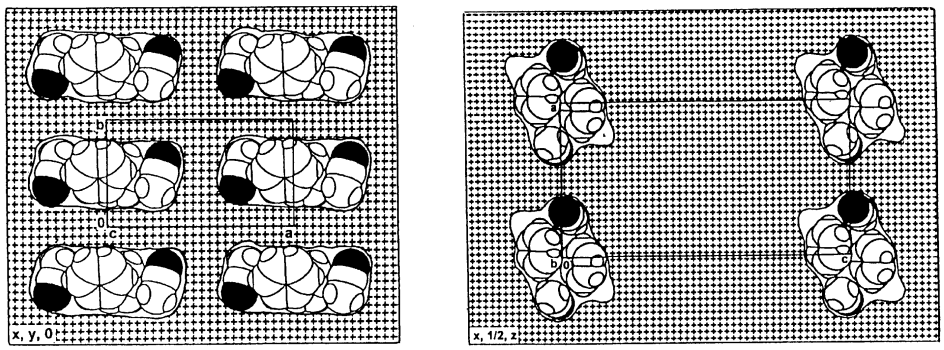

Figure 6. Cross section of **2** viewed (a) along [001] and (b) along [010]. The hatched region is that occupied by the host molecules. The guest molecules (with the nitrogen shaded) are located in the cavities.

C—H···O contacts, between 3.40Å and 3.55Å are observed. Intramolecular hydrogen bonds are present between O3 and O1, and between O2 and an adjacent phenyl ring. Details of these hydrogen bonds are given in Table II.

The calculated and experimental powder patterns of **1** are shown in Figure 2. These clearly match both in position in 2θ and in relative intensities. We frequently study the mode of decomposition of host-guest complexes, so it is valuable to know the structure of the non-porous form, as most inclusion compounds decompose to this same phase.

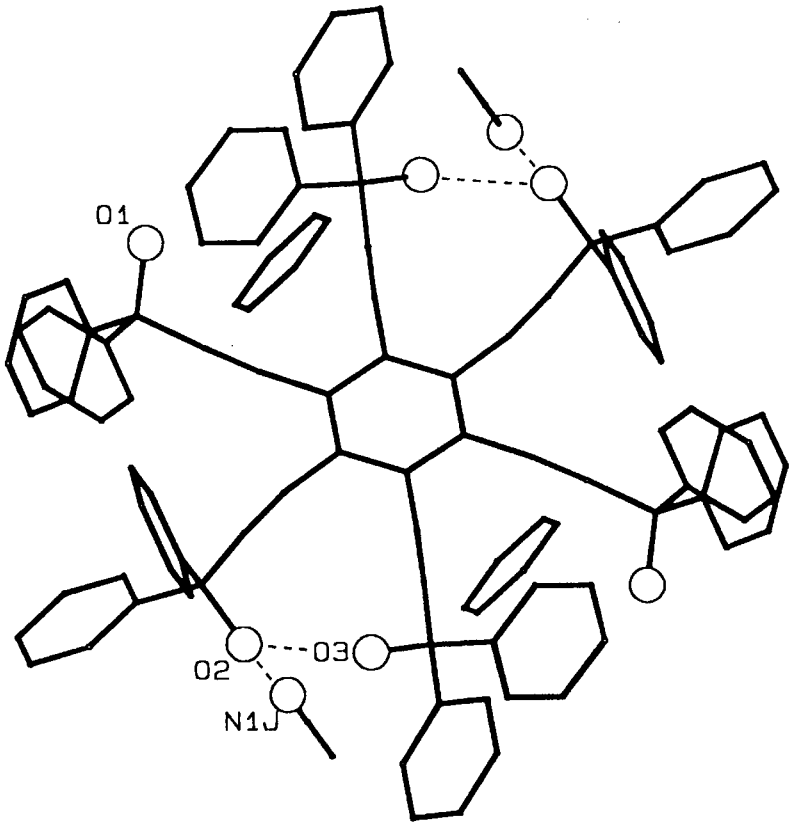

Figure 7. Hydrogen bonding scheme of **2**.

Crystals of **2** were obtained unexpectedly on crystallisation of **H** from a benzene solution, which was subsequently found to contain a small impurity of acetonitrile. Nuclear magnetic resonance spectroscopy and C, H, N elemental analysis were used to confirm the presence of the benzene and acetonitrile guests modelled in the crystal structure. The ^{1}H-NMR spectrum of **2** clearly shows two singlet peaks at δ = 2.03 and 7.37 ppm corresponding to the presence of acetonitrile and benzene, respectively. The elemental analysis results can be seen in Table III.

The thermograms for **2** are shown in Figure 3. The DSC curve shows a single endotherm at *ca* 92 °C. The host then melts with decomposition at 263 °C. The TG curve confirms the single step guest loss, and the host to guest ratio of 1 : 2 : 2 refined in the crystal structure (expected mass loss: 15.34%, observed mass loss: 14.88%). On desolvation the host framework collapses to the same α-phase as that of **1** (Figure 4). The hump-like shape of the experimental XRD powder pattern suggests that part of the sample may be amorphous. This can be explained by sample fragmentation, which may occur on desolvation, due to the difference in

solid reactant and product volumes, resulting in a loss of long range order resulting in products which are amorphous [10].

A simple competition experiment was carried out in order to determine the percentage acetonitrile impurity required in a benzene solution for the crystallisation of **2**. It was found that a *ca* 5% through to a *ca* 95% molar impurity resulted in the formation of **2**. Unfortunately, we have been unable to grow suitable crystals of the acetonitrile complex without benzene for diffraction studies. The crystals obtained are extremely thin needles, which are very unstable.

Compound **2** crystallises in the space group $P2_1/n$. The crystal packing is shown in Figure 5. The host molecules are packed in layers parallel to [010], with the central aromatic ring parallel to the (010) plane. The guest molecules are located in cavities between adjacent host molecules in each layer (Figure 6). An examination of the volume occupied by the guest molecules showed that these cavities are approximately $13 \times 6 \times 9$ Å. The acetonitrile guests are held in position by co-operative hydrogen bonding. The hydrogen bonds observed in **2** are detailed in Table IV, and illustrated in Figure 7.

It appears therefore, that the combination of benzene and acetonitrile guests is serendipitous, allowing for the formation of a stable inclusion compound with two guests. Benzene alone appears not to be included by **H**, resulting in the non-porous α-phase of **H**, while acetonitrile alone is included, but the resultant inclusion compound is very unstable. It may be that the inclusion of acetonitrile molecules forces the molecules in the α-phase sufficiently far apart to allow the intercalation of benzene molecules, which in turn stabilise the acetonitrile complex.

References

1. D.D. MacNicol and D.R. Wilson: *J. Chem. Soc., Chem. Commun*. 494 (1976).
2. For review see: D.D. MacNicol in *Inclusion Compounds*, Vol. 2, eds J.L. Atwood, J.E.D. Davies, D.D. MacNicol, Academic Press, London, chpt. 5 (1984); D.D. MacNicol and G.A. Downing in *Comprehensive Supramolecular Chemistry, Vol. 6, Solid State Supramolecular Chemistry: Crystal Engineering*, eds. D.D. MacNicol, F. Toda and R. Bishop, Pergamon Press, chpt. 14 (1996).
3. S.A. Bourne, M.R. Caira, L.R. Nassimbeni, M. Sakamoto, K. Tanaka and F. Toda: *J. Chem. Soc., Perkin Trans. 2* 1899 (1994).
4. S.A. Bourne, K.L. Gifford Nash and F. Toda: *J. Chem. Soc., Perkin Trans. 2* 2145 (1996).
5. S.A. Bourne, K.L. Gifford Nash and F. Toda: *Supramol. Chem*. **8**, 137 (1997).
6. G.M. Sheldrick: *Acta Crystallogr., Sect A*. **46**, 467 (1990).
7. G.M. Sheldrick: SHELXL-93, *J. Appl. Crystallogr*., in preparation.
8. K. Yvon, W. Jeitschko and E. Parthé: *J. Appl. Crystallogr*. **10**, 73 (1977).
9. F.H. Allen, O. Kennard, D.G. Watson, L. Brammer, A. G. Orpen and R. Taylor: *J. Chem. Soc., Perkin Trans. 2* S1 (1987).
10. D. Dollimore: *Thermochim. Acta*. **203**, 7 (1992).